Available online at www.sciencedirect.com
SCIENCE DIRECT
Journal of Power Sources 146 (2005) 594–597
JOURNAL OF POWER SOURCES
www.elsevier.com/locate/jpowsour

New layer-structured $LiNi_{1/3}Co_{1/3}Al_{1/3}O_2$ prepared via water-in-oil microemulsion method

Yu-Kai Lin [a], Chung-Hsin Lu [a,*], Hung-Chun Wu [b], Mo-Hua Yang [b]

[a] *Department of Chemical Engineering, National Taiwan University, Taipei, Taiwan 106, R.O.C.*
[b] *Materials Research Laboratories, ITRI, Chutung, Hsin-Chu, Taiwan 310, R.O.C.*

Available online 26 April 2005

Abstract

Nanosized $LiNi_{1/3}Co_{1/3}Al_{1/3}O_2$ with an α-$NaFeO_2$ structure has been successfully synthesized via a water-in-oil microemulsion method. Well-crystallized $LiNi_{1/3}Co_{1/3}Al_{1/3}O_2$ was obtained after heating at 800 °C for merely 3 h. The particle size of the microemulsion-derived powders was around 30 nm. The results of electrochemical analysis revealed that the synthesized powders exhibited higher discharge capacity at elevated temperatures than at room temperature. The Co^{3+}/Co^{4+} redox reactions are considered to play an important role in the discharge capacity and capacity retention of synthesized $LiNi_{1/3}Co_{1/3}Al_{1/3}O_2$.

Keywords: $LiNi_{1/3}Co_{1/3}Al_{1/3}O_2$; Microemulsion; Nanosize; Layered structure; Cathode materials

1. Introduction

In recent years, the $Li(Ni_xCo_{1-2x}Mn_x)O_2$ system used in lithium-ion batteries has been extensively investigated due to its high discharge capacity and good thermal stability [1–5]. $LiNi_{1/3}Co_{1/3}Mn_{1/3}O_2$ is a unique compound in this system because of its specific composition [2]. In $LiNi_{1/3}Co_{1/3}Mn_{1/3}O_2$, the valences of nickel, cobalt, and manganese ions are 2+, 3+, and 4+, respectively [6,7]. When $LiNi_{1/3}Co_{1/3}Mn_{1/3}O_2$ is cycled at a voltage ranging from 2.5 to 4.5 V, the redox reactions mainly occur on nickel ions [7]. If nickel and cobalt ions both serve as the redox centers, the electrochemical performance would be varied.

It is worthy to note that there are mainly two electrons (Ni^{2+}/Ni^{4+}) involved in this electrochemical reaction for $LiNi_{1/3}Co_{1/3}Mn_{1/3}O_2$ and valences of cobalt ions would not change significantly during the charge/discharge reactions. If the redox centers are not only located at nickel ions but also at cobalt ions, the electrochemical performance of the layer-structured materials might be varied. Therefore, aluminum ions are used to replace manganese ions in the layer-structured materials, and $LiNi_{1/3}Co_{1/3}Al_{1/3}O_2$ was synthesized in this study. Ohzuku et al. reported that rechargeable lithium ions in $LiAl_{1/4}Ni_{3/4}O_2$ were limited by the fraction of transition metal ions [8]. The redox centers in $LiNi_{1/3}Co_{1/3}Al_{1/3}O_2$ might be both nickel and cobalt ions during cycling. For layer-structured cathode materials, aluminum-ion doping has an advantage of improving the structural stability as well as the capacity retention [9,10]. In this study, $LiNi_{1/3}Co_{1/3}Al_{1/3}O_2$ powders were prepared using a microemulsion method. The phase formation and microstructural evolution of the prepared powders were examined. The electrochemical properties at room and elevated temperatures were also investigated.

2. Experimental

Lithium nitrate, nickel nitrate, cobalt nitrate, and aluminum nitrate were used as the starting materials. An aqueous solution was prepared by dissolving stoichiometric amounts of the above-mentioned nitrates in de-ionized water to form the water phase. Cyclohexane was chosen as the oil base. *n*-hexyl-alcohol and polyoxyethylene (10) octylphenyl ether (OP-10) were adopted as the co-surfactant and surfactant, re-

* Corresponding author.
E-mail address: chlu@ccms.ntu.edu.tw (C.-H. Lu).

0378-7753/$ – see front matter © 2005 Elsevier B.V. All rights reserved.
doi:10.1016/j.jpowsour.2005.03.044

spectively. The surfactant and co-surfactant were added into cyclohexane at a volume ratio of 3:2:10 to form the oil phase. Both aqueous and oil-phase solutions were mixed at a water-to-oil volume ratio of 1:10 to form stable transparent microemulsion solution, followed by dripping the microemulsion solution into hot kerosene at around 180 °C with a micropump to evaporate water. Then the oil solution containing micelles was dried in air at 480 °C for 3 h to remove residual oil and water for obtaining the precursor powders. After drying, the precursor powders were ground and further heated to a given temperature in a tubular furnace and calcined for various durations for synthesizing $LiNi_{1/3}Co_{1/3}Mn_{1/3}O_2$ powders.

X-ray diffraction (XRD) analysis using nickel-filtered Cu Kα radiation was performed to identify the crystalline phase. The morphology and particle size of the obtained powders were examined via transmission electron microscopy (TEM). The electrochemical characteristics of the reverse-microemulsion-derived powders were investigated in coin cells. The cathode composite was comprised of 85 wt.% $LiNi_{1/3}Co_{1/3}Al_{1/3}O_2$ powders calcined at 800 °C for 3 h, 5 wt.% KS6 graphite, 2 wt.% super-P carbon black, and 8 wt.% PVdF. Lithium foil was utilized as the anode, and the electrolyte solution was composed of 1 M $LiPF_6$ dissolving in EC/DEC (1:1 in v/v). The laboratory cells were assembled in the glove box and then galvanostatically cycled at the current density of 20 mA g^{-1} within the potential range of 2.5–4.5 V.

3. Results and discussion

Fig. 1 illustrates the X-ray diffraction patterns of the microemulsion-derived precursors of $LiNi_{1/3}Co_{1/3}Al_{1/3}O_2$ heated at (a) 480 °C for 3 h, (b) 700 °C for 3 h, (c) 800 °C for 1 h, and (d) 800 °C for 3 h. In Fig. 1(a), several diffraction peaks were observed, implying the formation of the crystallized compound during the drying process. On increasing the calcination temperature to 700 °C (see Fig. 1(b)), monophasic layered structure was obtained. The resulted powders were confirmed to have an α-$NaFeO_2$ structure belonging to the $R\bar{3}m$ space group. On further raising the calcination temperature to 800 °C (as shown in Fig. 1(c) and (d)), the diffraction peaks became sharpened and the (1 0 8) and (1 1 0) peaks clearly split, indicating the improvement of the crystallinity. It is confirmed that well-crystallized $LiNi_{1/3}Co_{1/3}Al_{1/3}O_2$ was obtained after calcination at 800 °C for 3 h.

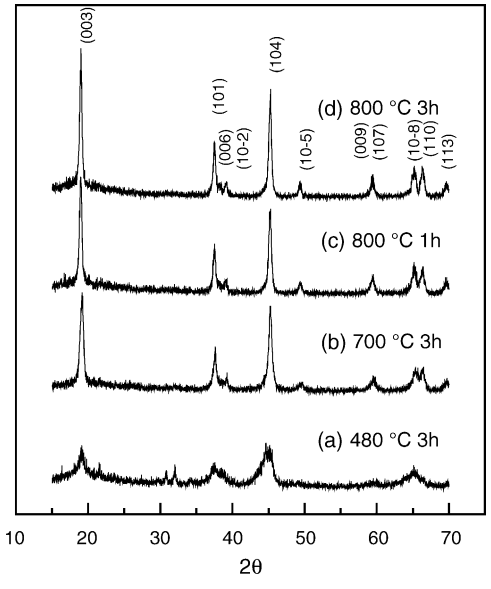

Fig. 1. X-ray diffraction patterns of (a) reverse-microemulsion-derived $LiNi_{1/3}Co_{1/3}Al_{1/3}O_2$ powders dried at 480 °C for 3 h, and the powders calcined at (b) 700 °C for 3 h, (c) 800 °C for 1 h, and (d) 800 °C for 3 h.

The lattice parameters of $LiNi_{1/3}Co_{1/3}Al_{1/3}O_2$ were calculated to be $a = 2.829(1)$ Å and $c = 14.186(5)$ Å using a least-square method. The substitution of manganese ions by aluminum ions in $LiNi_{1/3}Co_{1/3}Mn_{1/3}O_2$ led to a decrease in the lattice parameters in both *a*- and *c*-axis. This is because the radius of Al^{3+} cations ($r_{Al^{3+}} = 0.51$ Å) is smaller than that of Mn^{4+} ($r_{Mn^{4+}} = 0.53$ Å). Moreover, this substitution would render an increase in the average valence of nickel ions, leading to smaller cationic radius. Therefore, substituting Mn^{4+} by Al^{3+} resulted in decreased lattice parameters in both *a*- and *c*-axis.

Fig. 2 shows the (a) bright-field and (b) dark-field TEM images of $LiNi_{1/3}Co_{1/3}Mn_{1/3}O_2$ powders heated at 800 °C for 3 h. As shown in Fig. 2(a), the particle size of the sample was about 30 nm. The lightened particles in Fig. 2(b) indicate that well-crystallized sample was obtained. In addition, each particle is considered to be single crystal. This phenomenon may be attributed to the cage effect of water-in-oil microemulsion system [11].

Fig. 3 illustrates the charge/discharge curves and the discharge capacity versus cycle number of $LiNi_{1/3}Co_{1/3}Al_{1/3}O_2$ at room temperature and 55 °C. Curves I and II refer to the cells cycled within 2.5–4.5 V at room temperature and 55 °C, respectively. Curve III represents the cell measured within 2.5–4.2 V. These three charge curves displayed a distinct plateau during charging process at about 3.9 V, which was higher than that in $LiNi_{1/3}Co_{1/3}Mn_{1/3}O_2$. For curves I and II as shown in Fig. 3, during the first charging process ranging from 2.5 to 4.5 V, the charge capacities were 168.0 and 195.1 mAh g^{-1} at room temperature and 55 °C, respectively. If the amount of extractable lithium ions in $LiNi_{1/3}Co_{1/3}Al_{1/3}O_2$ is limited by the fraction of transition metal ions [8], the theoretical capacity of $LiNi_{1/3}Co_{1/3}Al_{1/3}O_2$ was calculated to be 205.1 mAh g^{-1}. Therefore, the first charge capacities at room temperature in curve I and at 55 °C in curve II were 82 and 95% of the theoretical value, respectively. This implies that most lithium ions can be extracted at high temperature upon charging between 2.5 and 4.5 V. On the other hand, when the upper cut-off voltage was lowered to 4.2 V (see curve III), the charge capacity was reduced to 130.7 mAh g^{-1} approx-

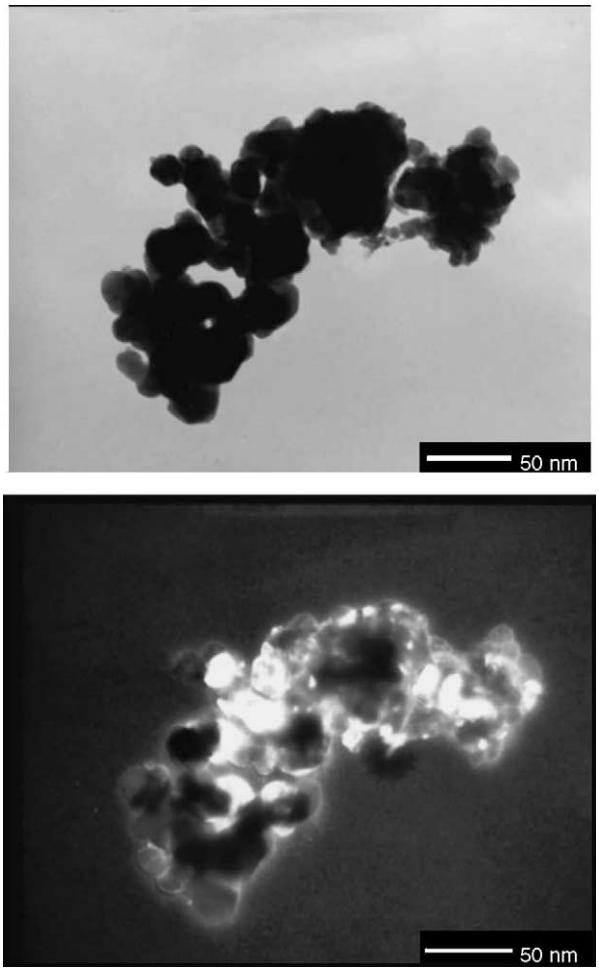

Fig. 2. (a) Bright-field and (b) dark-field TEM images of reverse-microemulsion-derived $LiNi_{1/3}Co_{1/3}Al_{1/3}O_2$ calcined at 800 °C for 3 h.

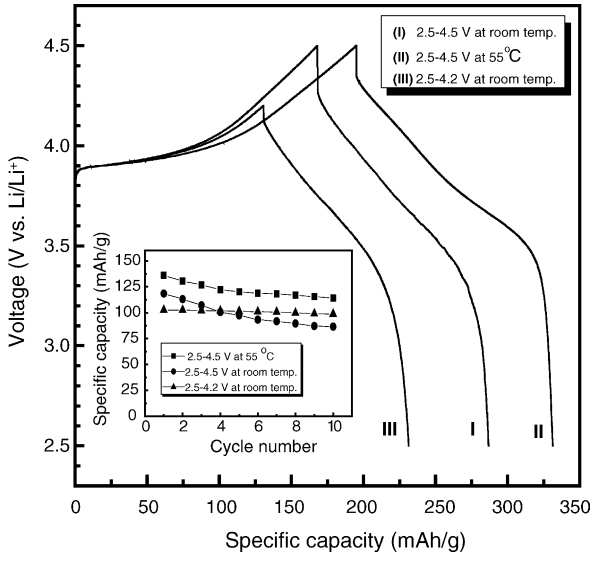

Fig. 3. Initial charge/discharge curves of reverse-microemulsion-derived $LiNi_{1/3}Co_{1/3}Mn_{1/3}O_2$ measured under 20 mA g^{-1} within (I) 2.5–4.5 V at room temperature, (II) 2.5–4.5 V at 55 °C, and (III) 2.5–4.2 V at room temperature. Inset: the plot of discharge capacity vs. cycle number.

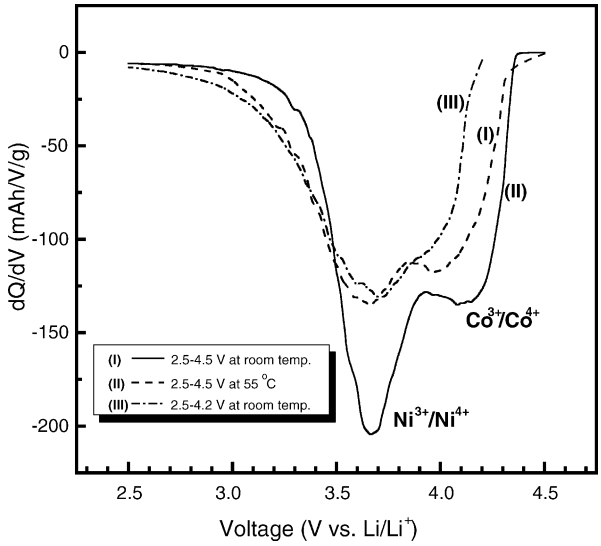

Fig. 4. Differential specific discharge capacity vs. potential for $Li/LiNi_{1/3}Co_{1/3}Al_{1/3}O_2$ measured within (I) 2.5–4.5 V at room temperature, (II) 2.5–4.5 V at 55 °C, and (III) 2.5–4.2 V at room temperature.

imating merely 63% of the theoretical value. The inset in Fig. 3 illustrates the relation between discharge capacity and cycle number for $LiNi_{1/3}Co_{1/3}Al_{1/3}O_2$. When the cells were discharged within 2.5–4.5 V, the initial discharge capacities for cells cycled at room temperature and 55 °C were 118.7 and 136.2 mAh g^{-1}, respectively. After 10 cycles, 73 and 84% of the initial discharge capacities were retained for cells cycled at room temperature and 55 °C, respectively. The discharge capacity and capacity retention at 55 °C were substantially superior to those at room temperature when the cells were cycled within 2.5–4.5 V. On the other hand, when the cell was discharged within 2.5–4.2 V, the initial discharge capacity was reduced to 102.7 mAh g^{-1}. After 10 cycles, the discharge capacity retained 98.7 mAh g^{-1}.

In order to examine the discharge behavior of $LiNi_{1/3}Co_{1/3}Al_{1/3}O_2$, differential discharge capacity versus voltage for various cycling conditions were plotted in Fig. 4. When the cell was measured within 2.5–4.5 V at room temperature, two peaks were clearly observed as shown in curve I. The peaks at 3.7 and 4.1 V are considered to correspond to Ni^{3+}/Ni^{4+} and Co^{3+}/Co^{4+} reduction reactions, respectively. For the cell measured within 2.5–4.5 V at 55 °C, these two peaks became intense and sharpened as shown in curve II, implying that the redox reactions and the charge transfer reactions were enhanced at elevated temperatures. When the upper cut-off voltage was reduced to 4.2 V, the peak at 4.1 V became diminished as shown in curve III. This indicates that when the cell was measured within 2.5–4.2 V, the Co^{3+}/Co^{4+} redox reactions hardly took place, thereby resulting in a decrease in the discharge capacity as shown in Fig. 3. Theses results reveal that the Co^{3+}/Co^{4+} redox reactions at high potential play an important role in the

discharge capacity and capacity retention of synthesized $LiNi_{1/3}Co_{1/3}Al_{1/3}O_2$.

4. Conclusions

Nanosized and well-crystallized $LiNi_{1/3}Co_{1/3}Al_{1/3}O_2$ has been successfully synthesized via the reverse-microemulsion route at 800 °C for 3 h. The particle size of the microemulsion-derived powders was around 30 nm. $LiNi_{1/3}Co_{1/3}Al_{1/3}O_2$ had smaller lattice parameters than did $LiNi_{1/3}Co_{1/3}Mn_{1/3}O_2$ since aluminum ions were smaller than manganese ions in radius. The discharge capacity of $LiNi_{1/3}Co_{1/3}Al_{1/3}O_2$ at 55 °C was larger than that at room temperature. The obtained results reveal that the Co^{3+}/Co^{4+} redox reactions at high potential play an important role in the discharge capacity and capacity retention of synthesized $LiNi_{1/3}Co_{1/3}Al_{1/3}O_2$.

References

[1] Z. Lu, D.D. MacNeil, J.R. Dahn, Elecrtrochem. Solid-State Lett. 4 (12) (2001) A200.
[2] T. Ohzuku, Y. Makimura, Chem. Lett. 7 (2001) 642.
[3] D.D. MacNeil, Z. Lu, J.R. Dahn, J. Electrochem. Soc. 149 (10) (2002) A1332.
[4] N. Yabuuchi, T. Ohzuku, J. Power Sources 119–121 (2003) 171.
[5] I. Belharouak, Y.K. Sun, J. Liu, K. Amine, J. Power Sources 123 (2003) 247.
[6] K.M. Shaju, G.V. Subba Rao, B.V.R. Chowdari, Electrochim. Acta 48 (2002) 145.
[7] B.J. Hwang, Y.W. Tsai, D. Carlier, G. Ceder, Chem. Mater. 15 (2003) 3676.
[8] T. Ohzuku, A. Ueda, M. Kouguchi, J. Electrochem. Soc. 142 (1995) 4033.
[9] G. Ceder, Y.M. Chiang, D.R. Sadoway, M.K. Aydinol, Y.I. Jang, B. Huang, Nature 392 (1998) 694.
[10] T. Ohzuku, A. Ueda, M. Kouguchi, J. Electrochem. Soc. 142 (1995) 4033.
[11] M. Arturo, L. Quintela, J. Coll. Interf. Sci. 8 (2003) 137.